



HAL
open science

Spherically symmetric models with pressure: separating expansion from contraction and generalizing TOV condition

José Pedro Mimoso, Morgan Le Delliou, Filipe C. Mena

► To cite this version:

José Pedro Mimoso, Morgan Le Delliou, Filipe C. Mena. Spherically symmetric models with pressure: separating expansion from contraction and generalizing TOV condition. 2009. hal-00429054v2

HAL Id: hal-00429054

<https://hal.science/hal-00429054v2>

Preprint submitted on 30 Oct 2009 (v2), last revised 10 Jun 2010 (v3)

HAL is a multi-disciplinary open access archive for the deposit and dissemination of scientific research documents, whether they are published or not. The documents may come from teaching and research institutions in France or abroad, or from public or private research centers.

L'archive ouverte pluridisciplinaire **HAL**, est destinée au dépôt et à la diffusion de documents scientifiques de niveau recherche, publiés ou non, émanant des établissements d'enseignement et de recherche français ou étrangers, des laboratoires publics ou privés.

Spherically symmetric models with pressure: separating expansion from contraction and generalizing TOV condition

José P. Mimoso*

*Departamento de Física,
Faculdade de Ciências da Universidade de Lisboa
Centro de Física Teórica e Computacional,
Universidade de Lisboa
Av. Gama Pinto 2, 1649-003 Lisboa, Portugal*

Morgan Le Delliou†

*Instituto de Física Teórica UAM/CSIC,
Facultad de Ciencias, C-XI,
Universidad Autónoma de Madrid
Cantoblanco, 28049 Madrid SPAIN*

Filipe C. Mena‡

*Centro de Matemática
Universidade do Minho
Campus de Gualtar, 4710-057 Braga, Portugal
(Dated: Received 30/10/09; Accepted...)*

We investigate spherically symmetric perfect fluid spacetimes and discuss the existence and stability of a dividing shell separating expanding and collapsing regions. We perform a 3 + 1 splitting and obtain gauge invariant conditions relating the intrinsic spatial curvature of the shells to the ADM mass and to a function of the pressure which we introduce and that generalises the Tolman-Oppenheimer-Volkoff equilibrium condition. We analyse the particular cases of the Lemaitre-Tolman-Bondi dust models with a cosmological constant as an example of a Λ -CDM model and its generalization to contain a central perfect fluid core. These models provide simple, but physically interesting illustrations of our results.

PACS numbers: 98.80.-k, 98.80.Cq, 98.80.Jk, 95.30.Sf, 04.40.Nr, 04.20.Jb

I. INTRODUCTION

Models of structure formation generally assume that small local inhomogeneities grow due the gravitational instability, so that the overdensities collapse and eventually form the "bound" structures we observe in the present universe. Underlying this viewpoint is the idea that the collapse of the overdensities departs from the general expansion of the universe. This approach often relies on the idea that a small overdensity can be approached as a closed patch in an otherwise spatially flat Friedmann universe and it claims that Birkhoff's theorem justifies that, on the one hand, its evolution is independent from the outside universe, and, on the other hand, that the behaviour of the outside Friedmann universe is immune to the collapse of the closed patch (see e.g. [1–3]). The collapse of overdensities has been extensively studied and

most works have been focused on the study of the formation both of small structure (astrophysical objects) and of large-scale structure as the outcome of the growth of small perturbations in a cosmological context. The latter subject, comprises the relativistic and newtonian analysis of the evolution of the fluctuations (see e.g. [1–4]) and the study of the subsequent amplification of the growing modes into the non-linear regime resorting to numerical methods (see e.g. [5–8]). In the present work we consider spherically symmetric, inhomogeneous universes with pressure, and study the question of whether there exists a dividing shell separating expanding and collapsing regions. Our goal bears a connection to the general problem of assessing the influence of global physics into the local physics [9, 10]. One aspect of this problem which has always attracted great interest is the endeavour to explain the local inertial phenomena in a Machian sense (see e.g. [11, 12]) and, in fact, Brans-Dicke theory [13–16] stems from this problem.

Another related aspect has been the study of the influence of cosmic expansion on local systems. Einstein and Straus [17] were the first to study this problem by constructing a global solution which resulted from matching the spherically symmetric vacuum Schwarzschild solution to an expanding dust FLRW exterior across a hypersurface preserving the symmetry. Bonnor has made several investigations along this line (see e.g. [18]). In particu-

*Electronic address: jpmimoso@cii.fc.ul.pt

†Also at Centro de Física Teórica e Computacional, Universidade de Lisboa, Av. Gama Pinto 2, 1649-003 Lisboa, Portugal; Electronic address: Morgan.LeDelliou@uam.es, delliou@cii.fc.ul.pt

‡Also at Departamento de Matemática, Instituto Superior Técnico, 1049-001 Lisboa, Portugal; Electronic address: fmema@math.uminho.pt

lar, he co-presented an exact solution representing a local distribution of Electrically Counterpoised Dust embedded in an expanding universe with zero spatial curvature [19], showing that the distribution participates in the expansion. Among the generalisations of this model are settings which keep the spherical symmetry but generalise the interior source fields by considering for example Vaidya (see [20] and references therein) or Lemaître-Tolman-Bondi (LTB) spacetimes (see [21–25]). On a different context, Herrera and co-workers [26] have studied the "cracking" of compact objects in astrophysics using small anisotropic perturbations around spherically symmetric homogeneous fluids in equilibrium.

In this work we use a different approach from all the works described above. In one hand, by making use of a single coordinate patch, we do not have to handle the matching problem. On the other hand, our approach is not perturbative. We adopt the formalism which has been recently developed in a remarkable series of papers by Lasky and Lun using Generalised Painlevé-Gullstrand (hereafter GPG) coordinates [27–29]. We perform a 3+1 splitting and obtain gauge invariant conditions relating not only the intrinsic spatial curvature of the shells to the ADM mass¹, but also a function of the pressure which we introduce and that generalises the Tolman-Oppenheimer-Volkoff (TOV) equilibrium condition.

In particular, we consider that the existence of a spherical shell separating an expanding outer region from an inner region collapsing to the center of symmetry, depends essentially on two conditions. The first condition establishes that there is no matter exchange across the shell. The second condition establishes that the generalized TOV equation is satisfied on that shell, and hence that this shell is in some sort of equilibrium. The difference with respect to the original problem where the TOV equation was introduced for the first time is twofold. Our result does not rely on the assumption of a static equilibrium of the spherical distribution of matter, and consequently does not assume that all the internal spherical perfect fluid spherical shells are constrained to satisfy the TOV equation. In our case the generalized TOV equation is just satisfied at the dividing shell. Besides, the generalized TOV function depends on the spatial 3-curvature in a more general way than the original TOV equation. Furthermore, we shall characterise the dividing shell with kinematic quantities which provide a gauge invariant formulation of the problem.

In order to illustrate our results we will analyse some particular cases. The simplest example is provided by the well-known Lemaître-Tolman-Bondi dust models with a cosmological constant which can be seen as an example of a Λ -CDM model. A preliminary presentation of this work can be found in [31]. As a second case we consider generalizations of the previous model to contain a cen-

tral perfect fluid core. These models provide simple, but physically interesting illustrations of our results.

An outline of the paper is: (II) The GPG formalism of Lasky and Lun: 3+1 splitting and gauge invariants kinematical quantities. (III) Existence of a shell separating contraction from expansion: general conditions. (IV) Particular examples (A) Λ -CDM model (LTB with a cosmological constant). (B) Perfect fluid core in a Λ -CDM model. (V) Discussion of our results.

We shall use the following index convention: Greek indices $\alpha, \beta, \dots = 1, 2, 3$ while latin indices $a, b, \dots = 0, 1, 2, 3$.

II. 3+1 SPLITTING AND GAUGE INVARIANTS KINEMATICAL QUANTITIES

In this section we set the basic equations that we shall subsequently need. For comparison, we follow closely the formalism used by Lasky and Lun (LL) [28], while slightly generalising their derivations for the explicit presence of a cosmological constant Λ .

A. Metric and ADM splitting

We adopt the GPG coordinates of Ref. [28] and perform an ADM 3+1 splitting [32] in which the spherically symmetric line element assumes a perfect fluid timelike normalised flow $n_a := -\alpha \nabla_a t = [-\alpha, 0, 0, 0]$ ($n_a n^a = -1$), defining with its lapse $N = \alpha$ and its radial shift vector $N^\mu = (\beta, 0, 0)$, an evolution of the spatially curved three-metric ${}^3g_{\mu\nu} = \text{diag}\left(\frac{1}{1+E}, r^2, r^2 \sin^2 \theta\right)$ with time ($d\Omega^2 := d\theta^2 + \sin^2 \theta d\phi^2$),

$$ds^2 = -\alpha(t, r)^2 dt^2 + \frac{1}{1+E(t, r)} (\beta(t, r) dt + dr)^2 + r^2 d\Omega^2. \quad (\text{II.1})$$

The 3+1 approach uses the projection operators along and orthogonal to the flow

$$N_b^a := -n^a n_b, \quad h^{ab} := g^{ab} + n^a n^b. \quad (\text{II.2})$$

where h^{ab} is the 3-metric on the surface Σ normal to the flow. Those projectors are also used for covariant derivatives: Along the flow, the proper time derivative of any tensor X_{cd}^{ab} is

$$\dot{X}_{cd}^{ab} := n^e X_{cd;e}^{ab}, \quad (\text{II.3})$$

and in the orthogonal 3-surface, each component is projected with h

$$X_{\bar{c}\bar{d};\bar{e}}^{\bar{a}\bar{b}} := h_f^{\bar{a}} h_g^{\bar{b}} h_c^{\bar{c}} h_d^{\bar{d}} h_e^{\bar{e}} X_{ij;k}^{fg}. \quad (\text{II.4})$$

¹ also referred to as Misner-Sharp mass[30].

Then the covariant derivative of the flow, from its projections, is defined as

$$n_{a;b} = N_b^c n_{a;c} + n_{\bar{a};\bar{b}} = -n_b \dot{n}_a + \frac{1}{3} \Theta h_{ab} + \sigma_{ab} + \omega_{ab}, \quad (\text{II.5})$$

where the projection trace, the expansion of the flow, is $\Theta = n^a_{;\bar{a}}$, the rate of shear σ_{ab} is its symmetric trace-free part and its skew-symmetric part is the vorticity ω_{ab} .

For perfect fluids we have the Raychaudhuri propagation equation

$$\begin{aligned} \dot{\Theta} - \dot{n}^a_{;\bar{a}} = & -\frac{1}{3} \Theta^2 + \dot{n}^a \dot{n}_a - \sigma_{ab} \sigma^{ab} + \omega_{ab} \omega^{ab} \\ & - \frac{\kappa}{2} (\rho + 3P) + \Lambda. \end{aligned} \quad (\text{II.6})$$

where $\kappa = 8\pi$.

The extrinsic curvature $\Theta_{ab} := \frac{1}{2} \mathcal{L}_n h_{ab}$ gives²

$$\begin{aligned} \Theta^{ab} = & \text{diag} \left[0, -\frac{1+E}{\alpha} \aleph, -\frac{\beta}{\alpha r^3}, -\frac{\beta}{\alpha r^3 \sin^2 \theta} \right], \quad (\text{II.7}) \\ \text{with } \aleph = & \left[\beta' + \frac{1}{2} \frac{\dot{E} - \beta E'}{1+E} \right]. \end{aligned}$$

and³

$$\Theta = -\frac{(\beta r^2)'}{\alpha r^2} - \frac{1}{2} \frac{\mathcal{L}_n E}{1+E}, \quad (\text{II.8})$$

which leads to

$$a = \frac{1}{3} \frac{r}{\alpha} \left(\frac{\beta}{r} \right)' + \frac{1}{6} \frac{\mathcal{L}_n E}{1+E}. \quad (\text{II.9})$$

The 3-Ricci tensor on Σ gives

$$\begin{aligned} {}^3R_{\mu\nu} = & \text{diag} \left[-\frac{E'}{(1+E)r}, -\frac{1}{2} E' r - E, \right. \\ & \left. \left(-\frac{1}{2} E' r - E \right) \sin^2 \theta \right]. \end{aligned} \quad (\text{II.10})$$

Samely, the 3-Ricci trace and trace-free 3-Ricci tensor derive from the 3-metric as

$${}^3R = -2 \frac{(Er)'}{r^2} \quad (\text{II.11})$$

and,

$${}^3Q_{\mu\nu} := {}^3R_{\mu\nu} - \frac{1}{3} {}^3g_{\mu\nu} {}^3R \quad (\text{II.12})$$

$$\Rightarrow {}^3Q_{\nu}^{\mu} = \frac{1}{6} \frac{E'r - 2E}{r^2} P_{\nu}^{\mu} = q(t, r) P_{\nu}^{\mu} \quad (\text{II.13})$$

$$\Rightarrow q = \frac{r}{6} \left(\frac{E}{r^2} \right)' \quad (\text{II.14})$$

where P_{ν}^{μ} is $\text{diag}[-2, 1, 1]$.

The trace and trace-free Hessian of α write

$$\frac{1}{\alpha} D^{\mu} D_{\mu} \alpha = \frac{\sqrt{1+E}}{\alpha r^2} \left(r^2 \sqrt{1+E} \alpha' \right)' \quad (\text{II.15})$$

and,

$$\frac{1}{\alpha} D_{\mu} D_{\nu} \alpha - \frac{1}{3\alpha} {}^3g_{\mu\nu} D^c D_c \alpha = \epsilon(t, r) P_{\mu\nu} \quad (\text{II.16})$$

$$\text{with } \epsilon = -\frac{r\sqrt{1+E}}{3\alpha} \left(\frac{\sqrt{1+E}}{r} \alpha' \right)'. \quad (\text{II.17})$$

The Bianchi identity $T_{b;a}^a = 0$ can be projected along n^b giving:

$$n^b T_{b;a}^a = -\mathcal{L}_n \rho - (\rho + P) \Theta = 0. \quad (\text{II.18})$$

while projections orthogonal to n^b give the Euler equation

$$h_a^b T_{b;c}^c = \begin{pmatrix} \beta \\ 1 \\ 0 \\ 0 \end{pmatrix} \left(P' + (\rho + P) \frac{\alpha'}{\alpha} \right) = 0 \quad (\text{II.19})$$

$$\Rightarrow P' = -(\rho + P) \frac{\alpha'}{\alpha}. \quad (\text{II.20})$$

B. The Einstein Field Equations

It is well known that the ADM approach separates the ten Einstein Field Equations (EFE) into four constraints and six evolution equations. Spherical symmetry reduces them to 2+2 equations.

The Hamiltonian constraint reads, in the presence of a cosmological constant,

$${}^3R + \frac{2}{3} \Theta^2 - 6a^2 = 16\pi\rho + 2\Lambda, \quad (\text{II.21})$$

the momentum constraint, restricted to the radial direction by symmetry,

$$(r^3 a)' = -\frac{r^3}{3} \Theta' \quad (\text{II.22})$$

and the evolution equations can be reduced to⁴

$$-2\mathcal{L}_n \Theta - \frac{1}{2} {}^3R - \Theta^2 - 9a^2 + \frac{2}{\alpha} D^a D_a \alpha = 24\pi P - 3\Lambda, \quad (\text{II.23})$$

$$-\mathcal{L}_n a - a\Theta + \epsilon - q = 0. \quad (\text{II.24})$$

² Recall that for a scalar $\mathcal{L}_n = n^a \partial_a = \frac{1}{\alpha} \partial_t - \frac{\beta}{\alpha} \partial_r$; [28] called it K_{ab} but we preferred the Ellis convention.

³ Note that we obtain a sign for K and a different from that of Ref. [28].

⁴ Note the sign differences in front of the Lie derivatives terms compared with [28]; our results give a sign for \dot{H} which is consistent with the Raychaudhuri equation restricted to the FLRW case.

Using Eqs. (II.8) and (II.9) in Eq. (II.22), one can simplify the latter into

$$-\frac{\mathcal{L}_n E}{1+E} = 2\frac{\beta}{\alpha^2}\alpha'. \quad (\text{II.25})$$

Using the guidance that, from Eqs. (II.11) and (II.14), ${}^3R + 12q$ eliminates derivatives in E , we can further simplify the combination of (Eqs. (II.23) + 6(II.24)) $\times r^2/3$ with expressions from Eqs. (II.8,II.9,II.11,II.14,II.15) as

$$2r(1+E)(\ln\alpha)' - 8\pi Pr^2 + \Lambda r^2 + 2r\mathcal{L}_n\left(\frac{\beta}{\alpha}\right) - \left(\frac{\beta}{\alpha}\right)^2 = -E. \quad (\text{II.26})$$

Substitution of Eq. (II.26) into Eq. (II.21) $\times r^2/4$ yields, together with Eqs. (II.8,II.9,II.11,II.25, $r/2\times$ II.26), a Poisson-like equation which, integrated over r defines a Misner-Sharp mass function [30]

$$\begin{aligned} M' &= 4\pi\rho r^2 \\ \Rightarrow M &= 4\pi\int_0^r \rho x^2 dx = r^2(1+E)(\ln\alpha)' \\ &\quad - 4\pi Pr^3 + \frac{1}{3}\Lambda r^3 + r^2\mathcal{L}_n\left(\frac{\beta}{\alpha}\right), \end{aligned} \quad (\text{II.27})$$

which with Euler's Eq. (II.20) rewritten, for $P \neq -\rho$, leads to the expression

$$\frac{M}{r^2} + 4\pi Pr = \mathcal{L}_n\left(\frac{\beta}{\alpha}\right) + \frac{1}{3}\Lambda r - \frac{1+E}{\rho+P}P'. \quad (\text{II.28})$$

The evolution Eq. (II.26) can be recast to recognise the definition of (II.27):

$$E + 2\frac{M}{r} + \frac{1}{3}\Lambda r^2 = \left(\frac{\beta}{\alpha}\right)^2. \quad (\text{II.29})$$

With Euler's Eq. (II.20), the momentum Eq. (II.25) becomes

$$\mathcal{L}_n E = 2\frac{\beta}{\alpha}\frac{1+E}{\rho+P}P', \quad (\text{II.30})$$

while taking Eq. (II.29)'s Lie derivative and using (II.30) with $\mathcal{L}_n\frac{1}{r} = -\frac{\beta}{\alpha}\partial_r\frac{1}{r} = \frac{\beta}{\alpha}/r^2$, then $\frac{\beta}{\alpha}\times$ Eq. (II.28) reads

$$\mathcal{L}_n M = 4\pi Pr^2\frac{\beta}{\alpha}. \quad (\text{II.31})$$

Taking the positive (contracting) root of Eq. (II.29), the evolution Eqs. $\alpha\times$ (II.31) and $\alpha\times$ (II.30) for M and E can be written in term of time derivatives, expliciting the Lie derivative:

$$\dot{M} = \alpha(M' + 4\pi Pr^2)\sqrt{2\frac{M}{r} + \frac{1}{3}\Lambda r^2 + E}, \quad (\text{II.32})$$

$$\dot{E} = \alpha\left(E' + 2\frac{1+E}{\rho+P}P'\right)\sqrt{2\frac{M}{r} + \frac{1}{3}\Lambda r^2 + E}. \quad (\text{II.33})$$

This system is then closed with a choice of an equation of state.

C. Generalized LTB

Getting the metric (II.1) into the LTB form, as in [28], requires a coordinate transform so that $\beta dt + dr \propto dR$. Taking $t(T)$ and $r(T, R)$, we have then the condition

$$\beta\partial_T t + \partial_T r = 0, \quad (\text{II.34})$$

which becomes

$$\beta = -\dot{r}. \quad (\text{II.35})$$

Consequently, the line element (II.1) can be rewritten as

$$ds^2 = -\alpha(T, R)^2(\partial_T t)^2 dT^2 + \frac{(\partial_R r)^2}{1+E(T, R)} dR^2 + r^2 d\Omega^2, \quad (\text{II.36})$$

where $E(T, R) > -1$ and we can freely absorb the time function in the new time by choosing $t = T$. Using now $\dot{}$ and $'$ for ∂_T and ∂_R respectively, Eq. (II.29) now reads

$$\dot{r}^2 = \alpha^2\left(2\frac{M}{r} + \frac{1}{3}\Lambda r^2 + E\right) \quad (\text{II.37})$$

and Eq. (II.32) rewrites, using Eq. (II.35),

$$\dot{M} = \beta 4\pi Pr^2 = 4\pi Pr^2 \alpha \sqrt{2\frac{M}{r} + \frac{1}{3}\Lambda r^2 + E}, \quad (\text{II.38})$$

while Eq. (II.33) $\times r'$ rewrites

$$\dot{E} r' = 2\beta\frac{1+E}{\rho+P}P' = 2\frac{1+E}{\rho+P}P'\alpha\sqrt{2\frac{M}{r} + \frac{1}{3}\Lambda r^2 + E} \quad (\text{II.39})$$

and Euler's Eq. (II.20) $\times r'$ is unchanged

$$\frac{\alpha'}{\alpha} = -\frac{P'}{\rho+P}. \quad (\text{II.40})$$

D. Remarks on Λ

In all that precedes, the cosmological constant was kept explicit. However, from the EFEs, one can include its effects in the total density and pressure as that of a fluid with $\rho_\Lambda = -P_\Lambda = \frac{\Lambda}{\kappa}$. We then obtain expressions identical to Lasky & Lun [28]. It is interesting to note that the Misner-Sharp mass, in the explicit Λ formulation, is only referring to the initial, "Aless" mixture, while encompassing the gravitational effects of the presence of Λ . From Eq. (II.27) we can define the mass M_{tot} and pressure term $4\pi P_{tot}r^3$ for the sum of the total perfect fluid mixture plus Λ by taking Eq. (II.27) for a perfect fluid and setting $\Lambda = 0$. We can also interpret the sum of the total mass and pressure terms as the mass of an equivalent dust model M_{ed} . We can then integrate the

mass of Λ fluid and introduce the ‘‘Misner-Sharp mass’’ [30] pressure term for the Λ fluid:

$$M_{tot} + 4\pi P_{tot} r^3 = r^2 (1 + E) (\ln \alpha)' + r^2 \mathcal{L}_n \left(\frac{\beta}{\alpha} \right) \equiv M_{ed}, \quad (\text{II.41})$$

$$M_\Lambda = \frac{4\pi}{3} r^3 \rho_\Lambda = \frac{\Lambda}{6} r^3, \quad (\text{II.42})$$

$$4\pi P_\Lambda r^3 = -\frac{1}{2} \Lambda r^3. \quad (\text{II.43})$$

Thus we can rewrite the Misner-Sharp sum of the mass and pressure term from its components from Eq. (II.27)

:

$$M + 4\pi P r^3 = M_{tot} + 4\pi P_{tot} r^3 + \frac{1}{3} \Lambda r^3, \quad (\text{II.44})$$

$$M_\Lambda + 4\pi P_\Lambda r^3 = -\frac{1}{2} \Lambda r^3 + \frac{\Lambda}{6} r^3 = -\frac{1}{3} \Lambda r^3, \quad (\text{II.45})$$

so $M_{tot} = M + M_\Lambda$ and $P_{tot} = P + P_\Lambda$. In Sec. III, unless stated otherwise, we will use M , ρ and P to mean their *total values* while referring to the perfect-fluid-only values as M_{pf} , ρ_{pf} and P_{pf} . In addition, the mass evolution Eq. (II.31) refers to the ‘‘Aless’’ mixture mass and pressure. We can thus extrapolate that this mass conservation equation is valid for each component of minimally coupled fluid in the mixture: we thus have for independent fluids

$$M = \sum_{fluid\ i} M_i, \quad (\text{II.46})$$

$$P = \sum_{fluid\ i} P_i, \quad (\text{II.47})$$

$$\mathcal{L}_n M_i = 4\pi P_i r^2 \frac{\beta}{\alpha} = \pm 4\pi P_i r^2 \sqrt{2 \frac{M}{r} + E}. \quad (\text{II.48})$$

III. GEOMETRICAL AND PHYSICAL CONDITIONS FOR THE EXISTENCE OF A DIVIDING SHELL

In our spherical symmetric approach, we are looking for shells dividing expansion at all time from regions of mixed behaviour involving periods of collapse.

This leads to an investigation of the conditions for the dynamical separation of sections of matter trapped inside a dividing surface (physical condition). We will see that this approach is distinct from a purely kinematic separation of contraction from expansion (geometrical condition) and will express the physical condition using kinematic quantities.

A. Misner-Sharp mass conservation

In the previous section we have seen how the Misner-Sharp mass is evolving with the flow under Eq. (II.31).

We can thus define a surface for which this mass is conserved with respect to the flow:

$$\begin{aligned} \forall t, \mathcal{L}_n M(t, r_\star(t)) &= 0 \\ \Leftrightarrow \forall t, E &= -2 \frac{M}{r_\star}, \text{ or } P_\star = 0 \text{ or } r_\star = 0, \end{aligned} \quad (\text{III.1})$$

While the second case, $P = 0$, defines a dust-like layer in the perfect fluid mix, and the third case, $r = 0$, is trivial, we shall concentrate on the first case, $E = -2 \frac{M}{r}$. In this case, from Eq. (II.30) we get

$$\mathcal{L}_n E = \pm 2 \sqrt{2 \frac{M}{r} + E} \frac{1 + E}{\rho + P} P' = 0, \quad (\text{III.2})$$

so the shell is characterised by fixed curvature and Misner-Sharp mass. This implies that if a prescribed initial P and ρ distribution is given such that there exist a shell where

$$E_\star = -2 \frac{M_\star}{r_\star}, \quad (\text{III.3})$$

then this shell can locally separate inner and outer regions that can be expanding and contracting differently. We call the separating shell a ‘‘limit shell’’, and denote it with \star . In GPG coordinates the above condition is equivalent to $\frac{\beta}{\alpha} \Big|_\star = 0$, or to $\beta_\star = 0$. We can then use it to compute

$$\dot{r}_\star = -\frac{2M}{E} \alpha \left[\frac{\mathcal{L}_n M}{M} - \frac{\mathcal{L}_n E}{E} \right]_\star = 0, \quad (\text{III.4})$$

$$\ddot{r}_\star = -\frac{2M}{E} \alpha^2 \left[\frac{\mathcal{L}_n^2 M}{M} - \frac{\mathcal{L}_n^2 E}{E} \right]_\star, \quad (\text{III.5})$$

and

$$\mathcal{L}_n r = -\frac{\beta}{\alpha} \Rightarrow \mathcal{L}_n r_\star = 0, \quad (\text{III.6})$$

so the limit shell appears as a ‘‘turnaround’’⁵ shell, in terms of areal radius.

However, these conditions are coordinate dependent and give limited insight as to how they would express for different observers. This calls for a definition using gauge invariant quantities.

B. Expansion and Shear

Newtonian structure formation in spherical symmetry provides a natural limiting shell that is a locus separating at a given time expansion from collapse: the turnaround radius (see e.g.[33]). The definition of that locus is given

⁵ See discussion in [1, Section 19, p77]

by the vanishing of the expansion with respect to the flow. Nevertheless, this is not necessarily the case resulting from condition III.1. Let us first start from the previous mass flow definition and examine the corresponding expansion.

In GPG coordinates [28], defining the flow by the shift/lapse vector, we can compute the expansion (the trace of the symmetric part of the projected covariant derivative of the flow vector), using Eqs. (II.25,II.8):

$$\Theta = - \left(\frac{\beta}{\alpha} \right)' - 2 \frac{\beta}{\alpha} \frac{1}{r} \quad (\text{III.7})$$

At r_* (for $\frac{\beta}{\alpha} = 0$), we have non-zero expansion given by

$$\Theta_* = - \left(\frac{\beta}{\alpha} \right)'_* \quad (\text{III.8})$$

The shear can also be expressed here from Eqs. (II.9) and (II.25) as

$$a = \frac{1}{3} \left[\left(\frac{\beta}{\alpha} \right)' - \frac{\beta}{\alpha} \frac{1}{r} \right], \quad (\text{III.9})$$

and we can then relate shear and expansion as (using Eq. III.6)

$$r \left(\frac{\Theta}{3} + a \right) = - \frac{\beta}{\alpha} = \mathcal{L}_n r, \quad (\text{III.10})$$

so on the limit shell,

$$\Theta_* + 3a_* = 0 \Leftrightarrow (\mathcal{L}_n r)_* = 0. \quad (\text{III.11})$$

1. Generalising TOV

The TOV equation, following [28], emerges from Eq. (II.28) in the static case.

We now generalise the TOV equation by defining a functional gTOV from Eq. (II.28) as

$$\begin{aligned} \text{gTOV} &= \left[\frac{1+E}{\rho_{pf} + P_{pf}} P'_{pf} + 4\pi P_{pf} r + \frac{M_{pf}}{r^2} - \frac{1}{3} \Lambda r \right] \\ &= \left[\frac{1+E}{\rho + P} P' + 4\pi P r + \frac{M}{r^2} \right]. \end{aligned} \quad (\text{III.12})$$

The definitions (III.10), (II.28) and (III.12) combine to yield

$$\text{gTOV} = -r \left[\mathcal{L}_n \left(\frac{\Theta}{3} + a \right) - \left(\frac{\Theta}{3} + a \right)^2 \right] \quad (\text{III.13})$$

$$= -\mathcal{L}_n^2 r. \quad (\text{III.14})$$

We can then obtain local conditions that yield the TOV equation on the limit shell when

$$\begin{aligned} \text{gTOV}_* = 0 &\Leftrightarrow \mathcal{L}_n^2 r = 0 \\ &\Leftrightarrow \mathcal{L}_n \left(\frac{\Theta}{3} + a \right)_* = 0. \end{aligned} \quad (\text{III.15})$$

We can further express gTOV in a form that reminds of the FLRW Raychaudhuri equation by using $\langle \rho \rangle \equiv M/(4\pi r^3/3)$, i.e.

$$\text{gTOV} = \frac{1+E}{\rho + P} P' + \frac{4\pi}{3} r (\langle \rho \rangle + 3P), \quad (\text{III.16})$$

and for FLRW it reduces to

$$\text{gTOV}_{FL} = \frac{4\pi}{3} r (\rho + 3P) = -\ddot{r}. \quad (\text{III.17})$$

2. Dynamics of the limit shell

We have seen that we could define the limit shell by only setting $E_* = -2M_*/r_*$ (so $\beta_* = 0$), so that $\Theta_* = 3a_*$. Now, using Eqs. (II.29,II.32,II.33,III.12) we find

$$\left(\frac{\beta}{\alpha} \right)^{\cdot} = \beta \left(\frac{\beta}{\alpha} \right)' + \alpha \text{gTOV} \quad (\text{III.18})$$

$$\Rightarrow \dot{\beta} = \beta \left(\beta' - \beta \frac{\alpha'}{\alpha} + \frac{\dot{\alpha}}{\alpha} \right) + \alpha^2 \text{gTOV}, \quad (\text{III.19})$$

so on the limit shell, we have

$$\left(\frac{\beta}{\alpha} \right)^{\cdot}_* = \alpha \text{gTOV}_* \quad (\text{III.20})$$

$$\Rightarrow \dot{\beta}_* = \alpha^2 \text{gTOV}_*. \quad (\text{III.21})$$

Recall that, in the LTB frame, $\beta = -\dot{r}$, so this tells us

$$\ddot{r}_{LTB,*} = -\alpha^2 \text{gTOV}_*, \quad (\text{III.22})$$

and thus when $\text{gTOV}_* = 0$ that shell has no acceleration and is therefore really static, as expressed in the original TOV equation. For completeness, we can reëxpress Eq. (III.6) with Eqs. (II.31,II.30,III.12) in GPG coordinates:

$$\begin{aligned} \ddot{r}_{GPG,*} &= -\frac{2M}{E} \alpha^2 \left[\frac{\mathcal{L}_n^2 M}{M} - \frac{\mathcal{L}_n^2 E}{E} \right]_* \\ &= -\alpha^2 \left[\text{gTOV}_* - r_*^2 \frac{\text{gTOV}_*^2}{M_*} \right]. \end{aligned} \quad (\text{III.23})$$

3. Raychaudhuri expansion evolution

From Eqs. (II.21) and (II.23), with Λ included as a fluid component, we have in the GPG frame,

$$-2\mathcal{L}_n \Theta - \frac{2}{3} \Theta^2 - 12a^2 + \frac{2}{\alpha} D^k D_k \alpha = 8\pi (\rho + 3P), \quad (\text{III.24})$$

and on the limit shell, that reads

$$-\frac{2}{\alpha} \dot{\Theta}_* - 2\Theta_*^2 + \frac{2}{\alpha} D^k D_k \alpha_* = 8\pi (\rho + 3P), \quad (\text{III.25})$$

showing that this shell can still be dynamic. Using the Euler Eq. (II.20), the Hessian (II.15) gives

$$\frac{2}{\alpha} D^\gamma D_\gamma \alpha = \frac{1+E}{\rho+P} P' \left[\frac{E'}{1+E} - \frac{2(\alpha r^2)'}{\alpha r^2} \right] - 2 \left(\frac{1+E}{\rho+P} P' \right)'. \quad (\text{III.26})$$

Thus Eq. (III.24) reads

$$\begin{aligned} -\mathcal{L}_n \Theta - \Theta^2 - \frac{2\beta}{r\alpha} \left[2\Theta + \frac{3\beta}{r\alpha} \right] &= 4\pi(\rho + 3P) \\ -\frac{P'}{2(\rho+P)} E' + \left(\frac{1+E}{\rho+P} P' \right)' & \\ + \left(\frac{2}{r} - \frac{P'}{\rho+P} \right) \frac{1+E}{\rho+P} P' &. \end{aligned} \quad (\text{III.27})$$

Here, we can recognise the first term of TOV. On the limit shell the above equation reads

$$\begin{aligned} -\frac{1}{\alpha} \dot{\Theta}_* - \Theta_*^2 &= 4\pi(\rho + 3P) \\ -\frac{P'}{2(\rho+P)} E' + \left(\frac{1+E}{\rho+P} P' \right)' & \\ + \left(\frac{2}{r} - \frac{P'}{\rho+P} \right) \frac{1+E}{\rho+P} P' &, \end{aligned} \quad (\text{III.28})$$

and we recast the Raychaudhuri equation for the FLRW case

$$-\mathcal{L}_n \Theta - \frac{\Theta^2}{3} = 4\pi(\rho + 3P) \quad (\text{III.29})$$

$$= -3\dot{H} - 3H^2. \quad (\text{III.30})$$

4. Remarks on null expansion limit shells

We now explore the consequences of having, in addition to (III.11), the condition $\Theta_* = 0$ for the limit shell. In this case, the shear must also vanish on the shell and

$$\left(\frac{\beta}{\alpha} \right)'_* = 0, \quad (\text{III.31})$$

which constrains the gradient of the generalised velocity field β/α .

In addition, and most importantly, the Raychaudhuri Eq. (III.27) shows that an initially expansion-free dividing shell is not likely to remain so, and will drift radially. If we impose the vanishing of $\mathcal{L}_n \Theta$ in Eq. (III.24), we derive

$$\frac{1}{\alpha_*} D^k D_k \alpha_* = 4\pi(\rho + 3P)_*, \quad (\text{III.32})$$

which then translates into a thermodynamic condition on the second-order derivative of P , which should induce

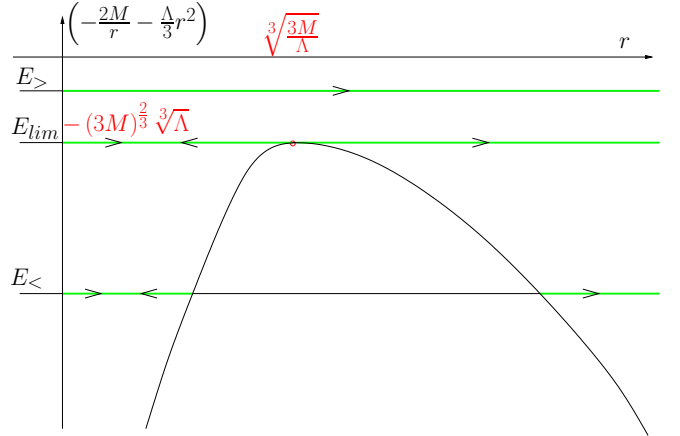


Figure 1: Kinematic analysis for a given shell of constant M and E . Depending on E relative to E_{lim} , the fate of the shell is either to remain bound ($E_< < E_{lim}$) or to escape and cosmologically expand ($E_> > E_{lim}$). There exists a critical behaviour where the shell will forever expand, but within a finite, bound radius ($E = E_{lim}$, $r \leq r_{lim}$)

a very specific and ad hoc local equation of state of the perfect fluid, namely

$$\begin{aligned} \left(\frac{1+E}{\rho+P} P' \right)'_* &= -4\pi(\rho + 3P)_* + \frac{P'_*}{2(\rho+P)_*} E'_* \\ - \left(\frac{2}{r} - \frac{P'}{\rho+P} \right)_* \frac{1+E_*}{\rho_*+P_*} P'_* &. \end{aligned} \quad (\text{III.33})$$

We conclude that the case of a static, expansion-free, limit shell is very restrictive: for example, in the simplest case, discussed below, of an inhomogeneous Λ -CDM model, Eq. (III.33) induces a restrictive equation of state $P = -\rho/3$ on the shell, which is neither verified by the dust component, nor by the Λ fluid, whereas the limit shell in this case derives from a staticity condition (see Sec. IV A).

IV. APPLICATIONS TO SIMPLE MODELS

We now will illustrate the behaviour according to the limit shell of simple models. First we will see how it appears in a Λ -CDM model, that is a Lemaitre-Tolman-Bondi dust model with a cosmological constant. We will then look at more general models including perfect fluids.

A. Overdensity in a Λ -CDM model

In what follows we consider a Λ -LTB model which, besides the bare LTB case, is exactly solvable, the most simple perfect fluid model with a cosmological context departing from LTB and which satisfies the conditions for the existence of an asymptotically r -static dividing shell. Indeed, as stated in [28], choosing $P = 0$ leads to

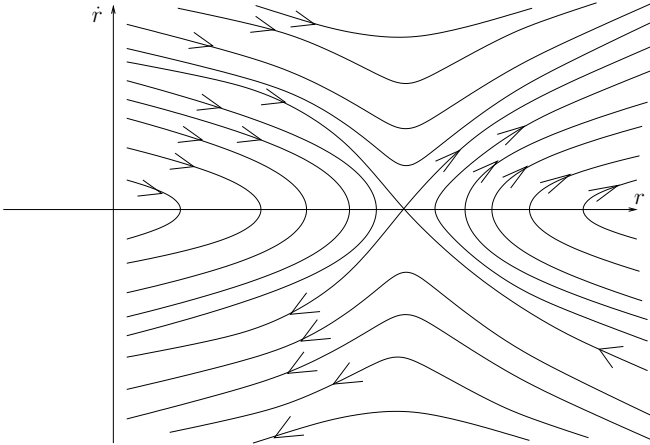


Figure 2: Phase space of a shell of fixed M and E . The scales are set by the value of $r_{lim} = \sqrt[3]{\frac{3M}{\Lambda}}$ while the actual kinematic of the shell is given by E .

the usual LTB solutions. Setting $P = 0$ in Eq. (II.38) implies⁶ $\dot{M} = 0$ and it is somewhat remarkable that this mass is still conserved for each shell in spite of the presence of Λ . Λ gives a homogeneous pressure, which in Eq. (II.40) gives $\alpha' = 0$ so we can redefine $\alpha dT = dT^*$ into the line element (II.36), and finally in Eq. (II.39), assuming no shell crossing $r' \neq 0$. We are therefore left with Eq. (II.37) in the classic LTB form, with

$$\dot{r}^2 = 2\frac{M}{r} + \frac{1}{3}\Lambda r^2 + E. \quad (\text{IV.1})$$

Adding a cosmological constant modifies the mass definition but not the dust equation of motion. However, we have an extra term that leads to a different dynamics. We can thus write the Raychaudhuri-like equation corresponding to time derivation of Eq. (IV.1):

$$\ddot{r} = -\frac{M}{r^2} + \frac{\Lambda}{3}r, \quad (\text{IV.2})$$

and this shows there exists a radius without acceleration for strictly positive Λ , contrary to pure dust. However, the first integral (IV.1) suffices for analysis of what happens to each shell (with fixed R).

1. Kinematic analysis

The Friedmann-like equation (IV.1) can be used to get the dynamics in a purely kinematical way. It can be expressed with a polynomial

$$\dot{r}^2 = \frac{\Lambda}{3r} \left(r^3 + \frac{3E}{\Lambda}r + \frac{6M}{\Lambda} \right) = \frac{\Lambda}{3r} P_{3,f}(r), \quad (\text{IV.3})$$

⁶ M can be understood as the mass of the dust alone but interacting with Λ , see Sec. IID.

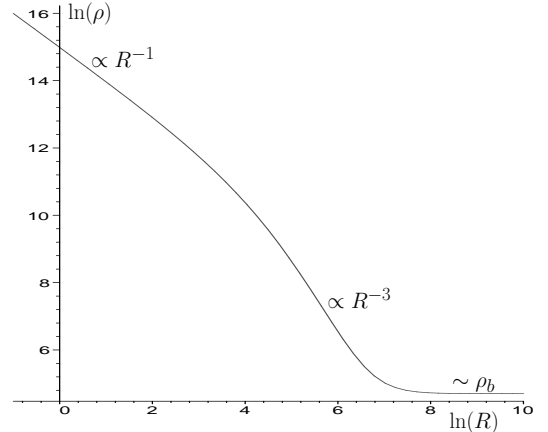


Figure 3: NFW with background density profile

which roots (given in appendix A) should obey the effective potential equation

$$E = V(r) \equiv -\frac{2M}{r} - \frac{\Lambda}{3}r^2. \quad (\text{IV.4})$$

Since $\dot{r}^2 \geq 0$, we have the condition

$$E \geq V(r). \quad (\text{IV.5})$$

The motion of a given shell over time thus follows $E = \text{const}$ curves above the effective potential V . Roots, the points of changing direction, translate as a geometric intersections between those curves and V . The effective potential admits one real negative root (0 energy/curvature) at

$$r = -\sqrt[3]{\frac{6M}{\Lambda}}, \quad (\text{IV.6})$$

and one double solution at its horizontal tangent ($V' = 0$)

$$r_{lim} = \sqrt[3]{\frac{3M}{\Lambda}}, \quad (\text{IV.7})$$

for which the value of E becomes

$$E_{lim} = -(3M)^{\frac{2}{3}} \Lambda^{\frac{1}{3}}. \quad (\text{IV.8})$$

It can be easily shown that any shell standing at r_{lim} with E_{lim} will automatically be a limit shell

$$r_{lim} = -\frac{2M_{tot,lim}}{E_{lim}} = -2\frac{M + \frac{\Lambda}{6}r_{lim}^3}{E_{lim}} = -\frac{3M}{E_{lim}}, \quad (\text{IV.9})$$

and calculating its gTOV, using the definition of Eq. (III.12) and recognising Eq. (IV.2),

$$\text{gTOV} = \frac{M}{r^2} - \frac{\Lambda}{3}r = -\ddot{r}, \quad (\text{IV.10})$$

that such a shell will be r -static ($\text{gTOV}_{lim} = -\ddot{r}_{lim} = 0$).

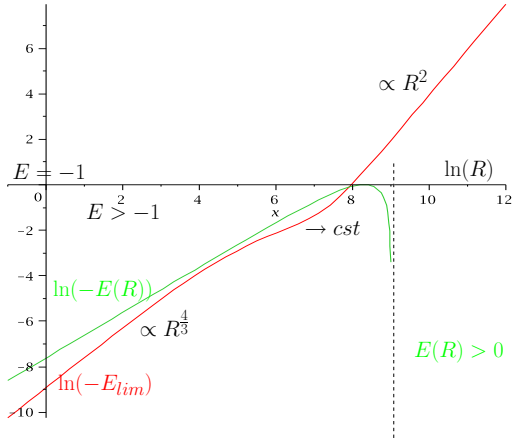


Figure 4: NFW with background E_{lim} and an example of E profile given by Eq. (IV.20), for $E_{min} = -1 + e^{-10}$ and $r_1 = e^9$.

The effective potential analysis is shown in fig. 1.

We can thus reconstruct the phase space of that shell in the (\dot{r}, r) plane. Above the energy E_{lim} , there is only one root in the negative region, thus the flow is qualitatively defined by its initial conditions. At E_{lim} , the double positive root gives a repulsive point, thus a saddle, while, below E_{lim} , the pair of roots give closed and open orbits as shown on fig. 2.

The Raychaudhuri-like equation can also be expressed with a polynomial

$$\ddot{r} = \frac{\Lambda}{3r^2} \left(r^3 - \frac{3M}{\Lambda} \right) = \frac{\Lambda}{3r^2} P_{3,R}(r), \quad (\text{IV.11})$$

admitting only one real root; the acceleration is always positive for

$$r \geq \sqrt[3]{\frac{3M}{\Lambda}}, \quad (\text{IV.12})$$

thus at infinity (cosmological constant dominates, M is monotonous in r). Therefore, at this root, there exist a limit radius beyond which there is no recollapse:

$$r_{lim}(R) = \sqrt[3]{\frac{3M(R)}{\Lambda}}. \quad (\text{IV.13})$$

Note that this radius corresponds to the saddle point, which initial energy radial profile is fixed with initial conditions for the mass distribution $E_{lim}(R) = -(3M(R))^{\frac{2}{3}} \Lambda^{\frac{1}{3}}$. Therefore the last intersection between the initial curvature profile, set by combining velocity and mass profiles, and this saddle point profile yields a global shell beyond which there is no recollapse, recovering separation of expansion from collapse. Explicit exact solutions for this ALTB evolution model are shown in appendix B. It is nevertheless crucial to realise that the selection of the limit shell from initial curvature does not entail necessarily that it should start as r -static. Indeed

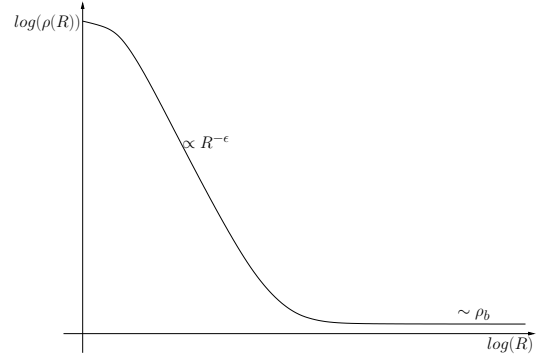


Figure 5: power law density profile without cusp and with background

the opposite should be true in general, as can be seen in Eqs. (IV.1) using E_{lim} , R_{lim} in (IV.4), and fig. 1: for any choice of the initial $R_{lim} < r_{lim}$, the radial velocity

$$\dot{R}_{lim}^2 = E_{lim} - V(R_{lim}) > 0, \quad (\text{IV.14})$$

so it appears that the r -static behaviour of the shell should only emerge asymptotically as it approaches zero velocity for infinite time. The selected limit shell therefore agrees with the conditions (III.11,III.15) only at infinity in time, and is traced back to initial conditions owing to the Λ +dust conservation of M and E in time. More general fluids should not always allow for this conservation on the limit shell, however once a shell verifies Eqs.(III.11,III.15), its staticity guaranties that it should verify it at time-infinity. It is remarkable that the existence of the limit shell only matters at time-infinity, suggesting that a weaker definition than (III.11,III.15) should be a sufficient condition.

2. Time dependent TOV

The shape of Eq. (IV.10) shows that, at the root of the Raychaudhuri-like polynomial, $\text{gTOV} = 0$ and that it is positive inside and negative outside. The trapped region is thus characterised by $\text{gTOV} \geq 0$. We can also compute, using $M = 4\pi \langle \rho \rangle r^3/3$,

$$\text{gTOV}' = \left[4\pi \left(\rho - \frac{2}{3} \langle \rho \rangle \right) - \frac{\Lambda}{3} \right] r' \quad (\text{IV.15})$$

so TOV is a decreasing function of r (for $r' > 0$, a fair assumption as seen when $r(t=0) = R$), except in regions where $\rho > \frac{2}{3} (\langle \rho \rangle + \rho_\Lambda)$, that is in density peaks. It is also a time dependent function through the evolution of r :

$$\text{gTOV} = \mp \left(\frac{2M}{r^3} + \frac{\Lambda}{3} \right) \sqrt{E + \frac{2M}{r} + \frac{\Lambda}{3} r^2}, \quad (\text{IV.16})$$

thus for a given shell, it increases with time for ingoing dust shells and decreases for outgoing ones. The main point is that with dust, turnaround shells have r -static

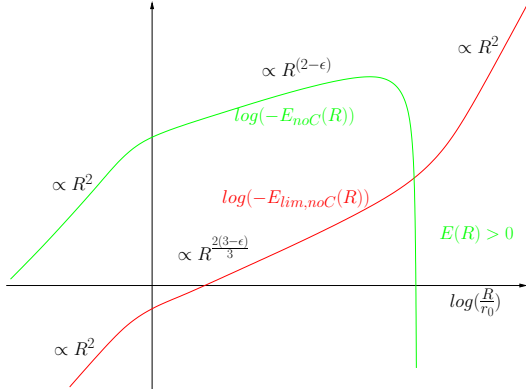


Figure 6: power law density without cusp + background $\ln(-E_{lim}) - \log(R)$ and $\log(-E) - \log(R)$ scales

gTOV, and that balanced shells (between their mass pull and that of Λ) verify the TOV equation and are thus static.

3. Examples of initial density

It is obvious then that initial conditions are crucial to determine the existence of a separating shell in the ALTB model since they set the profile of E and that of E_{lim} . A single crossing of the two curves ensures locally the existence of such a shell, while its global effect remains if the initial conditions do not foster shell crossing. This is the case if there is only one crossing from bound to unbound E s of E_{lim} . More complicated cases will be examined in a future work. We now proceed with examples of initial density profiles and then deduct the conditions on the corresponding curvature profile for a limit shell to exist.

a. NFW with background: The choice of an NFW [34] density profile is motivated by their prevalence in large cosmological dark matter haloes ([35, and references therein]). If we initialise the halo with such a density profile, with concentration $1/R_0$ and inflexion density $\rho_0/4$, placed on a constant background ρ_b , we can compute the corresponding mass profile. The density profile, as illustrated on fig. 3, is given by [34]

$$\rho = \frac{\rho_0}{\frac{R}{R_0} \left(1 + \frac{R}{R_0}\right)^2} + \rho_b. \quad (\text{IV.17})$$

The corresponding mass then reads

$$M = 4\pi \left\{ r_0^3 \rho_0 \left[\ln \left(1 + \frac{R}{r_0} \right) - \frac{R}{R+r_0} \right] + \rho_b \frac{R^3}{3} \right\}. \quad (\text{IV.18})$$

Now armed with the expression for the maximum energy function, the double root solution above, we can obtain from Eq. (IV.8) the bound upper limit for the initial Energy/cosmological profile that separates between ever

expanding and bound shells

$$E_{lim} = - (12\pi)^{\frac{2}{3}} \Lambda^{\frac{1}{3}} \left\{ r_0^3 \rho_0 \left[\ln \left(1 + \frac{R}{r_0} \right) - \frac{R}{R+r_0} \right] + \rho_b \frac{R^3}{3} \right\}^{\frac{2}{3}}. \quad (\text{IV.19})$$

Figure 4 shows that profile corresponding to the NFW with background mass. We then propose an example for the $E(R)$ profile, motivated by its cosmological Friedmann asymptotic curvature and its simple radial evolution from bound to unbound, as

$$E(R) = -4E_{min} \left(\frac{R}{r_1} \right) \left(1 - \frac{R}{r_1} \right), \quad (\text{IV.20})$$

where $r_1 > 0$ and $-1 < E_{min} < 0$, chosen so that E crosses E_{lim} near its constant density region. With the asymptotic constant density and Friedmann negative curvature ($E \simeq \frac{4}{r_1^2} R^2 = -k_\infty R^2$), these initial conditions model well a collapsing structure in an open background of curvature radius $\frac{r_1}{2}$. The resulting curves are shown in fig. 4. We have here an example where shells with $E < E_{lim}$ are trapped inside the limit shell defined by the intersection of the two profiles. Moreover, that limit shell in the case of dust with Λ has been shown to be static. Thus, with this set of physically motivated initial conditions, the limit shell defined in this way delimits a constant region of collapsing mass, separated from expanding shells.

b. Cosmological background with power law overdensity: The most natural cosmological initial condition is a power law overdensity, with or without cusp, upon a uniform background with an initial Hubble flow ([35]). The uniform background and initial Hubble flow ensures the asymptotic solution starts FLRW. In this second example of initial conditions, we explored both density profiles but illustrate only the cusplless case as it is more observationally sounded ([35, and refs. therein]). The density profiles, as illustrated for the second case on fig. 5, are given by ($\epsilon > 0$, and in the first case $\epsilon \leq 3$ for a finite central mass)

$$\rho = \rho_0 \left(\frac{R}{R_0} \right)^{-\epsilon} + \rho_b, \quad (\text{IV.21})$$

$$\rho = \rho_0 \left(1 + \frac{R}{R_0} \right)^{-\epsilon} + \rho_b. \quad (\text{IV.22})$$

Observations of the Cosmic Microwave Background (CMB) would imply to chose initial time at recombination and amplitudes of the order of $\rho_0 \sim 10^{-5} \rho_b$ ([see 35, and refs. therein]). The corresponding mass then reads, for the cuspy profile,

$$M_{cusp} = 4\pi r_0^3 \rho_0 \left\{ \begin{array}{l} \left[\ln \left(\frac{R}{r_0} \right) \right], \quad \epsilon = 3 \\ \left[\frac{\left(\frac{R}{r_0} \right)^{3-\epsilon}}{3-\epsilon} \right], \quad 0 < \epsilon < 3 \end{array} \right\} + \frac{4\pi}{3} \rho_b R^3, \quad (\text{IV.23})$$

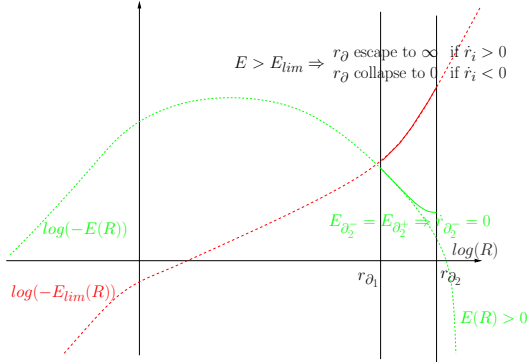


Figure 7: $r_{lim} < r_{\partial_1} < r_{\partial_2}$ case for a dust layer with Λ . Full space Λ -CDM diagram for $\log(-E_{lim}) - \log(R)$ and $\log(-E) - \log(R)$ in dashed line. This region is characterised by $E > E_{lim}$, so the dynamical analysis of fig. 1 yields continuation of initial velocities directions.

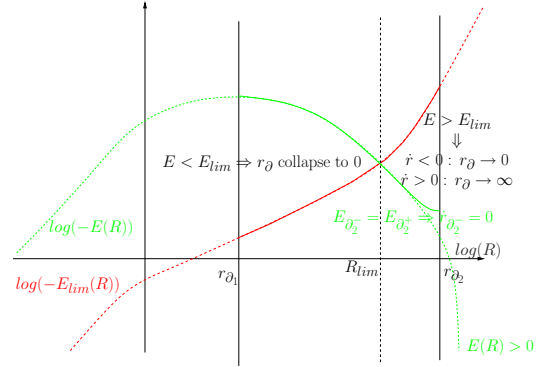


Figure 8: $r_{\partial_1} < r_{lim} < r_{\partial_2}$ case for a dust layer with Λ , Λ -CDM for $\log(-E_{lim}) - \log(R)$ and $\log(-E) - \log(R)$ in dashed line. The region with $E < E_{lim}$ is trapped by its set of effective potentials and will recollapse, that with $E > E_{lim}$, so the dynamical analysis of fig. 1 yields continuation of initial velocities. Separating shell remains in between those regions.

and for the profile with constant density in the centre

$$M_{noCusp} = 4\pi r_0^3 \rho_0 \times \begin{cases} \left[\frac{1}{2} \left(\frac{R}{r_0} \right) \left(\frac{R}{r_0} - 2 \right) + \ln \left(1 + \frac{R}{r_0} \right) \right], & \epsilon = 1 \\ \left[\left(\frac{R}{r_0} \right) \frac{2 + \frac{R}{r_0}}{1 + \frac{R}{r_0}} - 2 \ln \left(1 + \frac{R}{r_0} \right) \right], & \epsilon = 2 \\ \left[\frac{\frac{R}{r_0}}{\left(1 + \frac{R}{r_0} \right)^2} + \ln \left(1 + \frac{R}{r_0} \right) \right], & \epsilon = 3 \\ \left[\frac{\left(1 + \frac{R}{r_0} \right)^{3-\epsilon} - 1}{3-\epsilon} - 2 \frac{\left(1 + \frac{R}{r_0} \right)^{2-\epsilon} - 1}{2-\epsilon} + \frac{\left(1 + \frac{R}{r_0} \right)^{1-\epsilon} - 1}{1-\epsilon} \right], & \epsilon > 0 \end{cases} + \frac{4\pi}{3} \rho_b R^3. \quad (\text{IV.24})$$

The resulting boundary profile for E again follows Eq. (IV.8), using the obtained mass profiles. Taking an initial Hubble flow, $\dot{R} = H_i R$, the $E(R)$ profile is then defined by Eq. (IV.1) to be

$$E(R) = \left(H_i^2 - \frac{\Lambda}{3} \right) R^2 - \frac{2M}{R}. \quad (\text{IV.25})$$

The resulting comparison between E and E_{lim} for the non-cuspy case is shown in fig. 6. Once again, the intersection defines a static limit shell for which $r_{lim} = -\frac{2M_{tot,lim}}{E_{lim}}$ and $g_{TOV} = 0$, all shells inside it are in the kinematically bound region of fig. 1 while those outside are in the free region. Initial conditions ensure they will expand in a quasi FLRW manner.

These examples illustrate that cosmologically motivated initial conditions lead to a clear separation between expanding and collapsing regions. Therefore for these systems, expansion ignores the effects of collapse and conversely the details of the collapsing region can ignore the presence of a background expanding universe.

B. Perfect fluid core in a Λ -CDM model

Before examining the possibility of existence for a limit shell inside a perfect fluid in a sequel paper, where we shall present an ansatz for a perfect fluid inhomogeneous core in a Friedmann environment, let us turn to the configuration where a perfect fluid ball is surrounded by a) vacuum with a cosmological constant, b) dust and Λ .

1. Pure Λ exterior

In the same way as [28] did for a perfect fluid surrounded by a $\Lambda = 0$ vacuum, We can examine the interface between the perfect fluid and the Λ vacuum. In the latter region, both *the pressure radial derivative* $P' = 0$ *and the sum* $\rho_\Lambda + P_\Lambda = 0$ *for all time and place by definition of* Λ . In the same way as [28] showed for such a configuration with $\Lambda = 0$ vacuum, such a simple interface implies, through Eqs. (II.40) and (II.30), that the energy and lapse functions, E and α , are undefined there. These equations show that only if the fluid's pressure radial derivative P' vanishes faster than $\rho + P$ can E and α remain defined. This condition sets an unusual boundary constraint to the perfect fluid's EoS (simple linear EoS do not agree with it), but it is more fruitful to point out that such behaviour mimics that of a vanishingly thin layer of Λ -dust. Thus, the transition between the two regimes give rise to an inescapable Λ -dust atmosphere, however vanishingly thin, as was found in the pure vacuum case [28]. We have two free boundaries, $r_{\partial_1}(t)$ where the pressure vanishes and $r_{\partial_2}(t) > r_{\partial_1}(t)$ where the density vanishes, at which the EoS is defined as

$$0 = \begin{cases} f(\rho, P) & \text{for } r \in [0; r_{\partial_1}] \\ P & \text{for } r \in [r_{\partial_1}; r_{\partial_2}]. \end{cases} \quad (\text{IV.26})$$

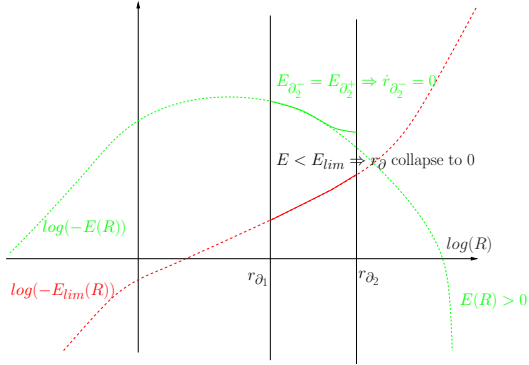


Figure 9: $r_{\partial_1} < r_{\partial_2} < r_{lim}$ case for a dust layer with Λ , Λ -CDM for $\log(-E_{lim}) - \log(R)$ and $\log(-E) - \log(R)$ in dashed line. This region is characterised by $E < E_{lim}$, so the dynamical analysis of fig. 1 yields eventual recollapse.

Evolution of $r_{\partial_1}(t)$ and $r_{\partial_2}(t)$ follows from setting respectively $P = 0$, then $P = \rho = 0$ in Eqs. (II.32), (II.33) and (II.40) to evolve those radii from initial conditions. The continuity of the curvature through both boundaries imposes again

$$\left[\lim_{r \rightarrow r_{\partial_i}^+} - \lim_{r \rightarrow r_{\partial_i}^-} \right] \{E(t, r)\} = 0, \quad (\text{IV.27})$$

that can be used to transmit the value of the mass parameter from the outer Schwarzschild-de Sitter spacetime down to the perfect fluid boundary curvature.

2. Limit shell

At this stage, the possibility opens for a limit shell in the Λ -CDM atmosphere of the core, provided that such shell verifies in conjunction Eqs. (III.3), or equivalently (III.11), and (III.15), which is only possible in a positively curved region. Given the surrounding Schwarzschild-de Sitter environment, the positive curvature requirement is at least locally filled near the outer boundary. There the analysis of Sec. (IV A) applies fully to yield, given initial conditions, the location of the previously discussed static virtual shell. Recall that in the Schwarzschild-de Sitter region, $E = -\frac{2M_{\partial_2}}{r} - \frac{\Lambda}{3}r^2$ while $E_{lim} = -(3M_{\partial_2})^{\frac{2}{3}} \Lambda^{\frac{1}{3}} = cst$, however the analysis only applies in the presence of dust, thus between r_{∂_1} and r_{∂_2} . Owing to the preservation of continuity in M and E at r_{∂_1} , whichever behaviour the perfect fluid may have, it will be confined by that of the previously explored Λ -CDM at its boundary.

Let us exhibit examples of such configurations: we can start from a similar example as presented in Sec. (IV A 3). Nevertheless, to preserve curvature continuity (IV.27), the initial velocity at r_{∂_2} should go to 0, and therefore the previous E profile should be modified accordingly. Then we are faced with three possibilities

due to the location of the dust layer boundaries compared with the limit shell in the full space dust model: $r_{lim} < r_{\partial_1} < r_{\partial_2}$, $r_{\partial_1} < r_{lim} < r_{\partial_2}$ or $r_{\partial_1} < r_{\partial_2} < r_{lim}$. Those cases are illustrated respectively on figs. 7, 8 and 9. In the first case, the dust layer locates above the maximum of their effective potential (IV.4) so their initial velocities gives the direction of their unhindered asymptotic behaviour, i.e. an initially expanding dust layer should expand forever. If a separating shell exists, it should lie within the perfect fluid region. The second case shows the existence of a separating shell, the perfect fluid being bound by the eventual recollapse of the r_{∂_1} shell, while some of the dust shell will expand through the vacuum region and eventually squeeze it to infinity. In the third case all the dust shells locate below the maximum of their effective potential (IV.4) so the whole mass will eventually recollapse, as if the separating shell was virtually located in the vacuum region.

Now sending the r_{∂_2} boundary to infinity, we can expand the dust layer accordingly and so long as Sec. (IV A)'s analysis yields a limit shell within the dust region, the perfect fluid shall be contained by the collapsing inner boundary (i.e. the third case disappear and we are left with cases $r_{lim} < r_{\partial_1}$ and $r_{\partial_1} < r_{lim}$ as treated in figs. 7 and 8).

In this section we have found that the presence of a cosmological constant does not modify the need for a dust layer around a perfect fluid core surrounded by vacuum. We have also given examples of limit shell separation behaviours for appropriately set initial conditions in the dust layer with Λ . We have even hinted at that possibility inside the perfect fluid from the dust behaviour, although such study should be left for a sequel paper.

V. SUMMARY AND DISCUSSION

In the present work we have considered spherically symmetric, inhomogeneous universes in order to ascertain under which conditions a dividing shell separating expanding and collapsing regions exists. This endeavour is important in relation with the present understanding of structure formation as the outcome of gravitational collapse of overdense patches within an overall expanding universe.

We have addressed this problematic by resorting to an ADM 3+1 splitting, utilising the so-called Generalized-Painlevé-Gullstrand coordinates as developed in Refs. [27, 28]. This enables us to follow a non-perturbative approach and to avoid having to consider the matching of the two regions with the contrasting behaviours. We have found local conditions characterising the existence of a dividing shell. We have related these conditions to a gauge invariant definition of the properties of the dividing shell. These require the vanishing of a linear combination of the expansion scalar and of the shear on the shell, as well as that of its flow derivative. In GPG coordinates, it summarises as a vanishing of both

first and second order flow derivatives of the areal radius.

In order to illustrate our findings we have considered some simple examples of cosmological interest that provide realizations of our results. We have considered a Λ -CDM model whereby we consider an LTB universe with dust and a cosmological constant. Notice that the simultaneous consideration of the latter two components yields a perfect fluid model for the combined matter content. Moreover it can be seen as simplified model of a dust universe within a cosmological setting coarsely provided by Λ which would then mimic the energy content of the background cosmological model with a rate of expansion much smaller than that of the pure dust collapse.

We have chosen initial conditions motivated by cosmological considerations and have discussed the existence of a dividing shell for those cases. We have also generalised a result of Ref. [28] for the case where a cosmological constant is present, which states that a perfect fluid core embedded in a universe filled with a cosmological constant necessarily exhibits a dust transition between the perfect fluid inner region and the outer vacuum region. This permits to envisage this case as a generalization of the former Λ -CDM examples.

Finally we should mention that, a thorough discussion of global conditions represent a much harder problem, and remain an open problem since this involves the full characterisation of a partial differential equations problem with boundary conditions in an open domain.

Acknowledgments

The authors wish to thank José Fernando Pascual-Sanchez for bringing to their attention the work of the authors of Ref. [28], and for helpful discussions. The work of MLeD is supported by CSIC (Spain) under the contract JAEDoc072, with partial support from CICYT project FPA2006-05807, at the IFT, Universidad Autonoma de Madrid, Spain, and was also supported by FCT (Portugal) under the grant SFRH/BD/16630/2004, at the CFTC, Lisbon University, Portugal. FCM is supported by CMAT, Univ. Minho, and FCT project PTDC/MAT/108921/2008. JPM also wishes to thank FCT for the *plurianual* running grant of CFTC.

Appendix A: ROOTS OF $P_{3,f}(r)$

1. Roots for the polynomial

The roots (r_0 s) of Eq. (IV.3) proceed from the polynomial $P_{3,f}$. We change variable such that $r = u + v$ and use the extra degree of freedom to choose to rewrite

$P_{3,f} = 0$ such that

$$uv = -\frac{E}{\Lambda}, \quad (\text{A.1})$$

$$\left(u^3 + \frac{3M}{\Lambda}\right)^2 = \left(\frac{E}{\Lambda}\right)^3 + \left(\frac{3M}{\Lambda}\right)^2. \quad (\text{A.2})$$

Solutions for the latter second degree polynomial come naturally as

$$u^3 = \frac{-3M \pm \sqrt{\frac{E^3}{\Lambda} + (3M)^2}}{\Lambda} \quad (\text{A.3})$$

$$\Rightarrow u = \sqrt[3]{\frac{-3M \pm \sqrt{\frac{E^3}{\Lambda} + (3M)^2}}{\Lambda}} e^{i\frac{2\pi k}{3}}. \quad (\text{A.4})$$

We are left with six solutions for u and v , which are symmetrical and related by Eq. (A.1) so uv being real, choosing u^3 as the positive squareroot solution, the corresponding v^3 becomes the negative one while u and v are complex conjugate, so

$$uv = \sqrt[3]{\frac{(3M)^2 - \frac{E^3}{\Lambda} - (3M)^2}{\Lambda^2}} = -\frac{E}{\Lambda}, \quad (\text{A.5})$$

therefore the roots are:

$$r_{k=0,\pm 1} = \left(\sqrt[3]{-3M + \sqrt{\frac{E^3}{\Lambda} + (3M)^2}} e^{i\frac{2\pi k}{3}} + \sqrt[3]{-3M - \sqrt{\frac{E^3}{\Lambda} + (3M)^2}} e^{-i\frac{2\pi k}{3}} \right) / \Lambda^{\frac{1}{3}} \quad (\text{A.6})$$

2. Real root(s)

For the positive discriminant, $\Delta = \frac{E^3}{\Lambda} + (3M)^2$, there is only one real root for $k = 0$. A negative or null discriminant, yields again the real $k = 0$ root and two other real roots for $k = \pm 1$, since then $v = \bar{u}$. We are then left with the single real root, noting

$$a_0 = \sqrt[3]{-3M + \sqrt{\frac{E^3}{\Lambda} + (3M)^2}}, \quad (\text{A.7})$$

$$a_0^* = \sqrt[3]{-3M - \sqrt{\frac{E^3}{\Lambda} + (3M)^2}}, \quad (\text{A.8})$$

$$r_0 = \frac{a_0 + a_0^*}{\Lambda^{\frac{1}{3}}}, \quad (\text{A.9})$$

and, when $\frac{E^3}{\Lambda} + (3M)^2 \leq 0$, the two other real roots

$$a_{\pm} = \sqrt[3]{3M + i\sqrt{\frac{(-E)^3}{\Lambda} - (3M)^2(1 \mp i\sqrt{3})}}, \quad (\text{A.10})$$

$$\bar{a}_{\pm} = \sqrt[3]{3M - i\sqrt{\frac{(-E)^3}{\Lambda} - (3M)^2(1 \pm i\sqrt{3})}}, \quad (\text{A.11})$$

$$r_{\pm} = \frac{a_{\pm} + \bar{a}_{\pm}}{2\Lambda^{\frac{1}{3}}}, \quad (\text{A.12})$$

3. Signs of the real roots:

So as to order the roots, it is necessary to look at their sign. This is important as r should be positive, $r < 0$ being unphysical. Recall that $M, \Lambda > 0$ and $E > -1$. When $\Delta > 0$, i.e. when $E > -(3M)^{\frac{2}{3}}\Lambda^{\frac{1}{3}} = E_{lim}$, we have only one real root and $r_0 > 0 \Rightarrow a_0 > -a_0^*$. We always have $-a_0^* = \sqrt[3]{3M + \sqrt{\frac{E^3}{\Lambda} + (3M)^2}} > 0$. Supposing $a_0 > 0$ (and thus $a_0^3 > 0$) then $-a_0^{*3}a_0^3 = \frac{E^3}{\Lambda} > 0 \Leftrightarrow E > 0$. Therefore, with the hypothesis $E > 0$, the condition $r_0 > 0$ implies $a_0 > -a_0^* \Leftrightarrow a_0^3 > -a_0^{*3} \Leftrightarrow -3M > 3M!$ Hence for $E > 0$ we have $r_0 < 0$. Samely, for $0 \geq E > -(3M)^{\frac{2}{3}}\Lambda^{\frac{1}{3}}$, requesting $r_0 > 0$ implies $a_0 > -a_0^*$ while $-a_0^* > 0 \geq a_0!$ Therefore, $0 \geq E > -(3M)^{\frac{2}{3}}\Lambda^{\frac{1}{3}}$ always entails $r_0 < 0$ and we conclude that r_0 is always negative when $E > -(3M)^{\frac{2}{3}}\Lambda^{\frac{1}{3}}$. The case when $(3M)^2\Lambda < 1$ is more interesting as we have three real roots for $-1 < E \leq -(3M)^{\frac{2}{3}}\Lambda^{\frac{1}{3}}$. Let us use the solutions of Eq. (A.6) in the form

$$r_k = \frac{u_k + \bar{u}_k}{\Lambda^{\frac{1}{3}}} = \frac{2\Re(u_k)}{\Lambda^{\frac{1}{3}}}. \quad (\text{A.13})$$

We know that

$$u_k^3 = -3M + i\sqrt{\frac{(-E)^3}{\Lambda} - (3M)^2} \quad (\text{A.14})$$

so $\Im(u_k^3) \geq 0$ and $\Re(u_k^3) < 0$. We can then rewrite $u_k^3 = \rho e^{i\varphi_{k,3}}$ with $\rho^2 = \frac{(-E)^3}{\Lambda}$, and $\varphi_{k,3} \in [\frac{\pi}{2} + 2k\pi; \pi + 2k\pi]_{k \in \mathbb{Z}}$. The values of u_k are deduced as $u_k = \rho^{\frac{1}{3}} e^{i\varphi_k}$ with $\varphi_k = \frac{\varphi_{k,3}}{3}$: $\varphi_k \in [\frac{\pi}{6} + \frac{2k\pi}{3}; \frac{\pi}{3} + \frac{2k\pi}{3}]_{k \in \mathbb{Z}}$. Each u_k admits the same modulus, so the phases, each separated by $2\pi/3$, give us the ranges and the order in which each root lies. The results are the following:

$$\varphi_0 \in [\frac{\pi}{6}; \frac{\pi}{3}] \subset [0; \frac{\pi}{2}] \Rightarrow r_0 > 0, \quad (\text{A.15})$$

$$\varphi_+ \in [\pi - \frac{\pi}{6}; \pi] \subset [\frac{\pi}{2}; \pi] \Rightarrow r_+ < 0, \quad (\text{A.16})$$

$$\varphi_- \in [-\frac{\pi}{2}; -\frac{\pi}{3}] \subset [-\frac{\pi}{2}; 0] \Rightarrow r_- \geq 0, \quad (\text{A.17})$$

and the order of the cosine (since r_k involves the real part of u_k) yields $-r_+ \geq r_0 \geq r_- \geq 0$. This is agreeing

with the analysis of Sec. IV A 1 understanding that the negative root shifts from r_0 to r_+ through the $\Delta = 0$ point, and that below the horizontal tangent, r_0 is the exterior turning point while r_- gives the interior envelope of the effective potential.

The above solutions gives us then the explicit equations for the intersection of the effective potential with the current curvature involved in eq. IV.1.

Appendix B: EXACT SOLUTIONS FOR AN INHOMOGENEOUS Λ CDM

The equation of motion admits analytical solutions in terms of hyperelliptic integrals (see also Lemaître [36]). From Eq. (IV.1)

$$t = \int_R^r \sqrt{\frac{r}{Er + 2M + \frac{\Lambda}{3}r^3}} dr, \quad (\text{B.1})$$

however, in conformal time ($dt = r d\eta$)

$$\begin{aligned} r'^2 &= Er^2 + 2Mr + \frac{\Lambda}{3}r^4, \quad (\text{B.2}) \\ \Rightarrow \eta &= \int_R^r \frac{1}{\sqrt{Er^2 + 2Mr + \frac{\Lambda}{3}r^4}} dr = \int_R^r \frac{1}{\sqrt{P_4(r)}} dr \end{aligned} \quad (\text{B.3})$$

Given that the incomplete elliptic integral of the first kind is defined by

$$F(x, k) = \int_0^x \frac{dt}{\sqrt{(1-t^2)(1-k^2t^2)}} = \int_0^x \frac{dt}{\sqrt{P_F(t)}}, \quad (\text{B.4})$$

it is possible by a rational change of variable, $z = \frac{ax+b}{cx+d}$ to go from P_F to P_4 :

$$\begin{aligned} P_F(z(x)) &= ((c-a)x + (d-b))((c+a)x + (d+b)) \times \\ &\times ((c-ka)x + (d-kb))((c+ka)x + (d+kb)) / (cx+d)^4 \\ &= \frac{P_4(x)}{(cx+d)^4}. \end{aligned} \quad (\text{B.5})$$

The solutions are therefore following, using $cr + d = \frac{ad-bc}{(a-cz)}$ and $dr = \frac{ad-bc}{(a-cz)^2} dz$

$$\eta = \int_R^r \frac{1}{\sqrt{P_F(z)}} \frac{1}{(cr+d)^2} dr = \frac{F(\frac{ar+b}{cr+d}, k) - F(\frac{aR+b}{cR+d}, k)}{(ad-bc)} \quad (\text{B.6})$$

We then just need to find a, b, c, d, k in terms of E, M, Λ . We already have the roots of $P_4 = P_{3,f}r\frac{\Lambda}{3}$ from Appendix A and we can write from Eq. (B.5)

$$r_1 = -\frac{d-b}{c-a}, r_2 = -\frac{d+b}{c+a}, r_3 = -\frac{d-kb}{c-ka}, r_4 = -\frac{d+kb}{c+ka}. \quad (\text{B.7})$$

We can obtain expressions for d and b , isolating them in the first and second pairs of roots:

$$d = -\frac{r_1(c-a) + r_2(c+a)}{2}, \quad b = \frac{r_1(c-a) - r_2(c+a)}{2}, \quad (\text{B.8})$$

$$= -\frac{r_3(c-ka) + r_4(c+ka)}{2}, \quad = \frac{r_3(c-ka) - r_4(c+ka)}{2k}. \quad (\text{B.9})$$

Equating the two ways of writing $b+d$, we obtain a linear relation between c and a ,

$$c = \frac{r_3k(1-k) + r_4k(1+k) - 2kr_2}{r_3(1-k) + 2kr_2 - r_4(1+k)} a. \quad (\text{B.10})$$

Now recall that the factors of x^4 and x^0 in P_4 are respectively

$$(c^2 - a^2)(c^2 - k^2a^2) = \frac{\Lambda}{3}, \quad (\text{B.11})$$

$$r_1r_2r_3r_4 = 0. \quad (\text{B.12})$$

The cosmological constant means from Eq. (B.11) that neither $c = \pm a$ nor $c = \pm ka$, while Eq. (B.12) entails that one of the roots is 0. If we choose $r_4 = 0$, then we have $d = -kb$ and therefore, from Eqs. (B.8), $d + kb = 0$ yields

$$\frac{c}{a} = \frac{r_1(1-k) - r_2(1+k)}{r_1(1-k) + r_2(1+k)}, \quad (\text{B.13})$$

so with Eq. (B.10) and $r_4 = 0$, we obtain a third degree polynomial in k (recall $k \neq 1$ for non-degeneracy of P_F)

$$(k-1) \left\{ \left(k + \frac{2r_1r_2 - r_1r_3 - r_2r_3}{r_1r_3 - r_2r_3} \right)^2 + 1 - \left(\frac{2r_1r_2 - r_1r_3 - r_2r_3}{r_1r_3 - r_2r_3} \right)^2 \right\} = 0 \quad (\text{B.14})$$

$$\Rightarrow k = \frac{2r_1r_2 - r_1r_3 - r_2r_3}{r_2r_3 - r_1r_3} \pm \sqrt{\left(\frac{2r_1r_2 - r_1r_3 - r_2r_3}{r_1r_3 - r_2r_3} \right)^2 - 1}. \quad (\text{B.15})$$

We also can rewrite the condition (B.10) to obtain a with Eq. (B.11): the positivity of Λ in Eq. (B.11),

$$\frac{\Lambda}{3} = \frac{4k^2(1-k^2)^2 [(1-k)^2 r_3 + 4r_2k] [r_3 - r_2] r_2 r_3}{[2r_2k + (1-k)r_3]^4} a^4, \quad (\text{B.16})$$

imposes to choose $r_3 > r_2 > 0$, and thus

$$a = \pm [2r_2k + (1-k)r_3] \sqrt{\frac{\sqrt{3[(1-k)^2 r_3 + 4r_2k] [r_3 - r_2] r_2 r_3}}{2k|1-k^2|}}. \quad (\text{B.17})$$

We deduce then c from Eq. (B.10)

$$c = \pm k [(1-k)r_3 - 2r_2] \sqrt{\frac{\sqrt{3[(1-k)^2 r_3 + 4r_2k] [r_3 - r_2] r_2 r_3}}{2k|1-k^2|}}, \quad (\text{B.18})$$

derive b from including the solutions (B.17,B.10) in its expression in Eq. (B.8)

$$b = \mp \frac{[4r_2k + (1-k)^2 r_3] r_1 + [(1-k^2) r_3] r_2}{2} \times \sqrt{\frac{\sqrt{3[(1-k)^2 r_3 + 4r_2k] [r_3 - r_2] r_2 r_3}}{2k|1-k^2|}}, \quad (\text{B.19})$$

and obtain d with our choice of $r_4 = 0$ that induces $d = -kb$

$$d = \pm \frac{k [4r_2k + (1-k)^2 r_3] r_1 + k [(1-k^2) r_3] r_2}{2} \times \sqrt{\frac{\sqrt{3[(1-k)^2 r_3 + 4r_2k] [r_3 - r_2] r_2 r_3}}{2k|1-k^2|}}. \quad (\text{B.20})$$

Inputting the values of the roots from appendix A, and the values of the transformation coefficients a , b , c , and d into Eq. (B.21) yields the conformal time evolution solution, that can be related to the cosmic time according to

$$t = \int r d\eta = \int_R^r r \frac{\partial}{\partial r} \left(\frac{F(\frac{ar+b}{cr+d}, k)}{(ad-bc)} \right) dr. \quad (\text{B.21})$$

Therefore there is an analytic solution to the ALTB model (see also Lemaitre [36]).

[1] P. J. E. Peebles, *The Large-Scale Structure of the Universe*, (Princeton University Press, Princeton, 1981)
 [2] T. Padmanabhan, *The Formation of Structure in the*

Universe, (Cambridge University Press, Cambridge, 1993)

[3] C. Cattoen and M. Visser, *Class. Quant. Grav.* **22**, 4913

- (2005) [arXiv:gr-qc/0508045].
- [1] W. de Sitter, *B. A. N.*, **7** (1933) 97
 - [2] S. W. Hawking, *Astrophys. J.*, **145** (1966) 544.
 - [3] V. F. Mukhanov, H. A. Feldman and R. H. Brandenberger, *Phys. Rept.*, **215** (1992) 203.
 - [4] A. R. Liddle and D. H. Lyth, *Phys. Rept.*, **231** (1993) 1 [arXiv:astro-ph/9303019].
 - [5] F. Bernardeau, S. Colombi, E. Gaztanaga and R. Scoccimarro, *Phys. Rept.* **367** (2002) 1 [arXiv:astro-ph/0112551].
 - [6] D. F. Mota and C. van de Bruck, *Astron. Astrophys.* **421** (2004) 71 [arXiv:astro-ph/0401504].
 - [7] M. Le Delliou, *JCAP*, **0601** (2006) 021 [arXiv:astro-ph/0506200].
 - [8] I. Maor, *Int. J. Theor. Phys.* **46** (2007) 2274 [arXiv:astro-ph/0602441].
 - [9] G. F. R. Ellis, *Int. J. Mod. Phys. A* **17**, 2667 (2002) [arXiv:gr-qc/0102017].
 - [10] V. Faraoni and A. Jacques, *Phys. Rev. D* **76**, 063510 (2007) [arXiv:0707.1350 [gr-qc]].
 - [11] D. W. Sciama, *Mon. Not. Roy. Astron. Soc.*, **113** (1953) 34.
 - [12] R. H. Dicke, *Natur.*, **192** (1961) 440.
 - [13] C. Brans and R. H. Dicke, *Phys. Rev.*, **124** (1961) 925.
 - [14] J. D. Barrow and J. P. Mimoso, *Phys. Rev. D*, **50**, 3746 (1994).
 - [15] J. P. Mimoso and D. Wands, *Phys. Rev. D*, **51**, 477 (1995) [arXiv:gr-qc/9405025].
 - [16] H. Iguchi, T. Harada and F. C. Mena, *Class. Quant. Grav.* **22** (2005) 841 [arXiv:gr-qc/0405026].
 - [17] A. Einstein & E. G. Straus, *Rev. Mod. Phys.*, **17** (1945) 120; *ibid* **18**, 148
 - [18] W. B. Bonnor, *Mon. Not. Roy. Astron. Soc.*, **167** (1974) 55-61.
 - [19] W. B. Bonnor, *Mon. Not. Roy. Astron. Soc.*, **282** (1996) 1467-1469.
 - [20] F. Fayos, J. M. M. Senovilla & R. Torres, *Phys. Rev. D*, **54** (1996) 4862
 - [21] A. Krasinski, *Physics in an inhomogeneous universe* (Cambridge University Press, Cambridge 1997).
 - [22] A. Krasinski and C. Hellaby, *Phys. Rev. D* **65**: 023501 (2001)
 - [23] A. Krasinski and C. Hellaby, *Phys. Rev. D* **69**, 023502 (2004) [arXiv:gr-qc/0303016].
 - [24] C. Hellaby and A. Krasinski, *Phys. Rev. D* **73**, 023518 (2006) [arXiv:gr-qc/0510093].
 - [25] F. C. Mena, B. C. Nolan and R. Tavakol, *Phys. Rev. D* **70** (2004) 084030 [arXiv:gr-qc/0405041].
 - [26] A. Abreu, H. Hernandez & L. A. Nunez, *Class. Quant. Grav.*, **24** (2007) 4631-4645; Di Prisco, L. Herrera & V. Varela, *Gen. Rel. Grav.*, **29** (1997) 1239
 - [27] R. J. Adler, J. D. Bjorkem, P. Chen, and J. S. Liu *Am. J. Phys.* [ArXiv:gr-qc/0502040]
 - [28] P. D. Lasky, & A. W. C. Lun, *Phys. Rev D*, **74** (2006) 084013
 - [29] P. D. Lasky and A. W. C. Lun, *Phys. Rev. D* **75** (2007) 024031 [arXiv:gr-qc/0612007]; P. D. Lasky and A. W. C. Lun, *Phys. Rev. D* **75** (2007) 104010 [arXiv:0704.3634 [gr-qc]]; P. Lasky and A. Lun, arXiv:0711.4830 [gr-qc].
 - [30] C. W. Misner, & D. H. Sharp, *Phys. Rev. B*, **136** (1964) 571.
 - [31] M. Le Delliou and J. P. Mimoso, *AIP Conf. Proc.*, **1122**, 316 (2009) [arXiv:0903.4651 [gr-qc]].
 - [32] G. F. R. Ellis and H. van Elst, *NATO Adv. Study Inst. Ser. C. Math. Phys. Sci.*, **541** (1999) 1 [arXiv:gr-qc/9812046].
 - [33] M. Le Delliou, R. N. & Henriksen, *A&A*, **408** (2003) 27; and references therein.
 - [34] J. F. Navarro, C. S. Frenk and S. D. M. White, *Astrophys. J.*, **462**, 563 (1996).
 - [35] M. Le Delliou, 2001, PhD Thesis, Queen's University, Kingston, Canada.
 - [36] G. Lemaitre, de Bruxelles, *Ann. Soc. Sci. B.*, **A53**, 51 (1933), printed in *Gen. Rel. Grav.*, **29**, 5 (1997)
 - [37] D. R. Matravers and N. P. Humphreys, *Gen. Rel. Grav.*, **33**, 531 (2001) [arXiv:gr-qc/0009057].